


RESEARCH

Open Access



N^6 -methyladenosine modification of *CENPK* mRNA by ZC3H13 promotes cervical cancer stemness and chemoresistance

Xian Lin^{1,2,3†}, Feng Wang^{4†}, Jian Chen^{3†}, Jing Liu¹, Yi-Bin Lin¹, Li Li¹, Chuan-Ben Chen^{2*} and Qin Xu^{1*} 

Abstract

Background: Stemness and chemoresistance contribute to cervical cancer recurrence and metastasis. In the current study, we determined the relevant players and role of N^6 -methyladenine (m^6A) RNA methylation in cervical cancer progression.

Methods: The roles of m^6A RNA methylation and centromere protein K (*CENPK*) in cervical cancer were analyzed using bioinformatics analysis. Methylated RNA immunoprecipitation was adopted to detect m^6A modification of *CENPK* mRNA. Human cervical cancer clinical samples, cell lines, and xenografts were used for analyzing gene expression and function. Immunofluorescence staining and the tumorsphere formation, clonogenic, MTT, and EdU assays were performed to determine cell stemness, chemoresistance, migration, invasion, and proliferation in HeLa and SiHa cells, respectively. Western blot analysis, co-immunoprecipitation, chromatin immunoprecipitation, and luciferase reporter, cycloheximide chase, and cell fractionation assays were performed to elucidate the underlying mechanism.

Results: Bioinformatics analysis of public cancer datasets revealed firm links between m^6A modification patterns and cervical cancer prognosis, especially through ZC3H13-mediated m^6A modification of *CENPK* mRNA. *CENPK* expression was elevated in cervical cancer, associated with cancer recurrence, and independently predicts poor patient prognosis [hazard ratio = 1.413, 95% confidence interval = 1.078 – 1.853, $P = 0.012$]. Silencing of *CENPK* prolonged the overall survival time of cervical cancer-bearing mice and improved the response of cervical cancer tumors to chemotherapy in vivo ($P < 0.001$). We also showed that *CENPK* was directly bound to SOX6 and disrupted the interactions of *CENPK* with β -catenin, which promoted β -catenin expression and nuclear translocation, facilitated p53 ubiquitination, and led to activation of Wnt/ β -catenin signaling, but suppression of the p53 pathway. This dysregulation ultimately enhanced the tumorigenic pathways required for cell stemness, DNA damage repair pathways necessary for cisplatin/carboplatin resistance, epithelial-mesenchymal transition involved in metastasis, and DNA replication that drove tumor cell proliferation.

*Correspondence: ccb@fjmu.edu.cn; xuqinfj@163.com

[†]Xian Lin, Feng Wang, and Jian Chen have contributed equally to this work

¹ Departments of Gynecology, Fujian Cancer Hospital and Fujian Medical University Cancer Hospital, Fujian Medical University, Fuzhou 350014, China

² Department of Radiation Oncology, Fujian Cancer Hospital and Fujian Medical University Cancer Hospital, Fujian Medical University, Fuzhou 350014, China

Full list of author information is available at the end of the article



Conclusions: CENPK was shown to have an oncogenic role in cervical cancer and can thus serve as a prognostic indicator and novel target for cervical cancer treatment.

Keywords: *N*⁶-methyladenosine, Centromere protein K, Cervical cancer, Stemness, Chemoresistance

Background

Existing data have shown that cervical cancer ranks as the second leading cause of cancer-associated deaths among women 20–39 years of age [1, 2], with treatment failure and poor prognosis attributed to cervical cancer cell stemness, chemoresistance, and metastasis [3]. Identifying alternative targets therefore represents an urgent priority to best utilize these tumorigenic properties in cervical cancer.

Several recent studies have suggested that *N*⁶-methyladenine (*m*⁶A) RNA methylation, the most abundant RNA modification that functionally affects mRNAs, lncRNAs, and miRNAs, is also involved in cervical cancer progression [4–6]. Many proteins are known to contribute to the *m*⁶A RNA methylation process; specifically, ZC3H13, METTL3, WTAP, and others function as methyltransferases to catalyze the addition of *m*⁶A marks on RNA. In addition to methyltransferases, demethylases (e.g., FTO and ALKBH5) catalyze the removal of *m*⁶A marks from RNA, while *m*⁶A readers, such as YTHDF1/2/3, YTHDC1/2, IGF2BP1/2/3, and others bind RNA to recognize *m*⁶A marks [7, 8]. The biological roles in modulating cervical cancer progression are poorly understood for many *m*⁶A-related genes because of the effects in aberrant regulation of downstream signaling pathways.

Previous studies have suggested links between centromere protein K (CENPK) and the progression of malignant tumors, such as ovarian cancer, breast cancer, hepatocellular carcinoma, bladder cancer, oligodendrogliomas, and lung adenocarcinoma [9–14]. CENPK is a subunit of the centromeric complex involved in assembly of kinetochore proteins. In coordination with centromere protein A (CENPA) and other centromere components, CENPK is an essential protein in chromosome segregation and mitotic progression [15]. Despite this broad contribution to different cancers, the relationship between CENPK and cervical cancer remains unknown, and the mechanism by which CENPK dysregulates cancer progression has not been established.

The purpose of the current study was to establish a connection between specific *m*⁶A methylation patterns and cervical cancer survival rates and prognosis, and to determine the effect of relevant factors on cervical cancer cell stemness, chemoresistance, metastasis, and proliferation using cervical cancer cell lines, animal models, and clinical samples, as well as publicly available cancer

datasets. In particular, we focused on the mechanism by which hypermethylation of *CENPK* mRNA results in upregulation, leading to disruption of SOX6 interactions and dysregulation of downstream Wnt and p53 pathway targets. Herein, we proposed a novel regulatory axis that promoted the tumorigenic properties of cervical cancer cells arising from the *m*⁶A methyltransferase, ZC3H13, through CENPK/SOX6 to the Wnt/ β -catenin and p53 signaling pathways.

Methods

Cell cultures

Cervical cancer cell lines (HeLa and SiHa) were purchased from the Chinese Academy of Sciences Cell Bank (Shanghai, China) and cultivated in Dulbecco's modified Eagle medium (DMEM) containing 10% fetal bovine serum. Cervical cancer cells were grown at 37 °C with 5% CO₂ and 95% room air. Cells were routinely measured for *Mycoplasma* contamination.

Cell transfections

Lentiviral particles harboring shRNA targeting *CENPK* (sh-CENPK) and negative control shRNA (sh-NC) were designed and constructed by GeneChem Corporation (Shanghai, China). Lentivirus particles were transfected into cervical cancer cells using a polybrene reagent. Plasmids (ov- β -catenin and ov-CENPK) were designed and constructed by Vigene Biosciences Corporation (Shandong, China). *CENPK* siRNA (si-CENPK), *SOX6* siRNA (si-SOX6), *p53* siRNA (si-p53), and *ZC3H13* siRNA (si-ZC3H13) were obtained from RiboBio Corporation (Guangzhou, China) (Additional file 1: Table S1). Following the manufacturer's protocol, plasmids and siRNAs were transduced into cervical cancer cells using Lipofectamine™ 2000 (Invitrogen Corporation, Shanghai, China). After transfection for 48 h–72 h, cells were subjected to further experimentation.

Tumorsphere formation assay

The protocol for the tumorsphere formation assay was previously described [16]. Briefly, cervical cancer cells (5000 cells/well) were seeded on 6-well ultra-low-attachment plates (Corning, Inc., New York, NY, USA) and cultured in serum-free DMEM/F12 with 2% B27, 20 ng/ml of EGF, and 20 ng/ml of FGF. The tumorspheres were recorded and counted on day 14 post-seeding, and the

number and size of tumorspheres were analyzed after passaging for three generations.

MTT assay

Cervical cancer cells (1000 cells/well) were seeded onto 96-well plates. At the indicated time, MTT (5 mg/ml; Sigma-Aldrich Corporation, St. Louis, MO, USA) was added to each well. After a 4 h incubation, dimethyl sulfoxide (Sigma-Aldrich Corporation) was added to each well. The absorbance value (OD) of each well was detected at 490 nm.

Colony-formation assay

Cervical cancer cells were plated at a density of 100 cells per well to measure cell proliferation. After a 10 d culture, colonies were fixed with methanol and stained with a hematoxylin solution. The number of colonies (≥ 50 cells) was counted under a light microscope. Cervical cancer cells were treated with cisplatin or carboplatin for 6 h at the indicated concentrations before seeding at a concentration of 500 cells per well to assess cell chemoresistance, as previously described [17]. After a 10 d of incubation, the colonies were fixed, stained, and photographed for analysis.

Transwell assays

Transwell assays were used to evaluate the migration and invasion capacity of cervical cancer cells. Cells suspension were seeded to the upper chamber of Transwell plates coated with Matrigel (BD Biosciences, Franklin Lakes, NJ, USA) for invasion assays or non-coated for migration assays; DMEM supplemented with 10% FBS was added to the lower chambers. The migrated and invaded cells were fixed, stained, and photographed under light microscopy.

EdU incorporation assays

EdU assay was conducted using the Apollo567 in vitro imaging kit (RiboBio Corporation, Guangzhou, China) following the manufacturer's protocol. After a 2 h treatment with EdU (10 $\mu\text{mol/L}$), cervical cancer cells were fixed with 4% paraformaldehyde, permeabilized with 0.3% Triton X-100, and co-stained with Apollo fluorescent dyes and DAPI (5 $\mu\text{g/ml}$). The EdU-positive cells were recorded and calculated under fluorescence microscopy.

Immunofluorescence

Cervical cancer cells were seeded and grown on coverslips. After incubation, the cells were fixed with 4% paraformaldehyde, permeabilized with 0.2% Triton X-100, and incubated with antibodies (Additional file 1: Table S2). The cells were then co-stained with DAPI

(0.2 mg/ml) and photographed with a fluorescence confocal microscope.

Reverse transcription-polymerase chain reaction (RT-PCR) and quantitative real-time PCR (qPCR)

Total RNAs were extracted from cervical cancer cells or xenografts using TRIzol (Invitrogen Corporation), and cDNAs were generated using a reverse transcription reagent kit (TaKaRa Corporation, Dalian, China). The synthesized cDNAs were adopted as templates for RT-PCR and qPCR with specific primers on Bio-Rad T100 and Bio-Rad CFX 96 (Bio-Rad, Hercules, CA, USA), respectively. β -actin was used as a control. The images were visualized by Bio-Rad GelDoc XR⁺ for RT-PCR. Relative mRNA expression was quantified using the $2^{-\Delta\Delta\text{Ct}}$ method for qPCR.

Western blotting

Cervical cancer cells were lysed in lysis buffer, and proteins were quantified using a BCA protein assay kit (Thermo Scientific, Waltham, MA, USA). After loading, proteins were separated, transferred, and immunoprobed with specific antibodies. Antibodies against the following proteins were used: Flag; CENPK; ZC3H13; SOX6; β -catenin; c-Jun; c-Myc; CCND1; p53; p21; Vimentin; Ubiquitin; GAPDH; Histone; and β -actin. Detailed antibody information is shown in Additional file 1: Table S2. Chemiluminescence was used for protein detection, and the Bio-Rad ChemiDocTM CRS+ Molecular Imager was adopted for capturing images.

Animal studies

The Institutional Animal Ethical Committee, Experimental Animal Center of Fujian Medical University and Fujian Cancer Hospital approved the protocols for animal studies (K2020-036-01). All experiments conformed to all relevant regulatory standards. BALB/c-nu mice were grouped as follows to detect tumor growth: HeLa-sh-NC [mice inoculated with scramble shRNA-infected control HeLa cells ($n=5$)] and HeLa-sh-CENPK [mice inoculated with CENPK-targeted shRNA-infected HeLa cells ($n=5$)]. The mice were subcutaneously inoculated with 5×10^6 cells/100 μl in the flank. The longest and the shortest diameters of the growing tumors were measured every 3 d with a caliper, and the tumor volume (V) was counted by the following equation: $V = (\text{the longest diameter} \times \text{the shortest diameter}^2)/2$. The mice were grouped as follows to evaluate the tumor-initiating frequency and were inoculated with a series of 5×10^5 , 2×10^5 , and 5×10^4 cells subcutaneously: HeLa-sh-NC ($n=6$); and HeLa-sh-CENPK ($n=6$). The mice bearing subcutaneous xenograft tumors were grouped as follows to evaluate tumor chemoresistance: HeLa-sh-NC

($n=10$); HeLa-sh-CENPK ($n=10$); HeLa-sh-NC + cisplatin [mice inoculated with scramble shRNA-infected control HeLa cells and 3 mg/kg of cisplatin once a week intraperitoneally (ip) for 6 weeks ($n=10$)] [18, 19]; and HeLa-sh-CENPK + cisplatin [mice inoculated with CENPK-targeted shRNA-infected HeLa cells and ip cisplatin ($n=10$)]. Survival curves were plotted using Kaplan–Meier analyses. The detection of cervical cancer metastatic potential was performed using a pulmonary metastasis model. BALB/c-nu mice were grouped as follows and all mice were inoculated with 1×10^6 cells/100 μ l through the tail vein: HeLa-sh-NC ($n=5$); and HeLa-sh-CENPK ($n=5$). Four weeks after injection, the formation of lung metastasis was evaluated under light and fluorescent microscopy.

The group assignment was the same in the mice inoculated with SiHa cells except carboplatin (30 mg/kg, ip once a week for 4 weeks) [20] was substituted for cisplatin in the SiHa-sh-NC + carboplatin and SiHa-sh-CENPK + carboplatin groups. A total of 144 BALB/c-nu female mice (4–5-weeks-old) were used in this study.

Luciferase reporter assay

The assays were carried out, as described in our previous study [21]. The Wnt signaling and p53 signaling activity assays were carried out using the luciferase assay system. Cervical cancer cells were co-transfected with TOPFlash or FOPFlash with pRL (Millipore Corporation, Billerica, MA, USA) to detect Wnt signaling. Cervical cancer cells were transfected with pGL4 luciferase reporter vector (Promega Corporation, Madison, WI, USA) harboring a p53 response element to detect p53 signaling. Cervical cancer cells were transfected with pmirGLO luciferase reporter vector (Promega Corporation) harboring 3'-UTR of *CENPK* to detect the impact of ZC3H13 on *CENPK* transcriptional levels. After transfection for 48 h, cells were collected and subjected to luciferase activity measurement using the Dual-Luciferase Reporter Assay System (Promega Corporation) on a BioTek luminometer.

Co-immunoprecipitation (Co-IP)

Co-IP was performed with a Pierce Co-IP kit (Thermo Scientific, Shanghai, China), according to the manufacturer's instructions. Briefly, total proteins were lysed from cervical cancer cells and the protein concentration was quantified. Proteins (5 mg) were then incubated with specific antibodies or IgG, which was used as a negative control. The enriched proteins were eluted and used for Western blotting.

Chromatin immunoprecipitation (ChIP)

The ChIP assays were carried out with a ChIP assay kit (Thermo Scientific, Shanghai, China) according to the

manufacturer's instructions. Briefly, chromatin from cervical cancer cells was crosslinked, extracted, and clipped with *Micrococcal* Nuclease to generate DNA fragments. Immunoprecipitation was performed with specific antibodies (Additional file 1: Table S2) or IgG, which served as a negative control. The DNA fragments were eluted, purified, and subjected to PCR and/or qPCR.

Cycloheximide chase assay

The cycloheximide chase assay was performed as described in our previous study [22]. Cervical cancer cells were subjected to treatment with cycloheximide (50 μ g/ml) at the indicated time. Subsequently, proteins were collected and quantified using a BCA protein assay kit (Thermo Scientific, Waltham, MA, USA). The proteins were further subjected to Western blotting, and signals were recorded for evaluating the protein half-life.

Cell fractionation assay

The cell fractionation assay was carried out with NE-PER™ Nuclear and Cytoplasmic Extraction Reagents (Thermo Scientific, Shanghai, China), as described in our previous study [22]. Cervical cancer cells were sequentially treated with ice-cold CER I and the CER II extraction reagent. The supernatant containing cytoplasmic extract was collected after centrifugation. The pellet was further incubated with CER extraction reagent. After centrifugation, the supernatant containing nuclear extract was retained. The collected proteins were further subjected to Western blotting.

Methylated RNA immunoprecipitation (MeRIP)

According to the manufacturer's instructions, MeRIP was performed using a MeRIP m⁶A kit (Millipore Corporation). Briefly, RNAs were extracted from cervical cancer cells and subjected to fragmentation followed by immunoprecipitation with magnetic beads conjugated with m⁶A antibody or IgG, which served as a negative control. The enriched RNAs were subjected to reverse transcription after RNA elution and purification. The synthesized cDNAs were further analyzed by qPCR and/or PCR.

Patient tissues

One hundred-nineteen paraffin-embedded cervical cancer specimens and 35 paraffin-embedded adjacent normal tissues in tissue chips (HUteS154Su01) were purchased from Shanghai Outdo Biotech (Shanghai, China). All the patients underwent surgery and had a confirmed pathologic diagnosis. Clinical data were extracted from the patients' medical records. Some clinicopathological characteristics, such as histological grade and Ki67 status, were not available for all patients. Ethics approval and patient written consent were obtained from the

Ethics Committee of Shanghai Outdo Biotech Corporation (YB M-05-02). The procedures used in this study adhered to the tenets of the Declaration of Helsinki.

Immunohistochemistry (IHC)

Paraffin-fixed Sects. (4 μm) from tissues were subjected to deparaffinization, rehydration, and antigen retrieval in citrate buffer. After eradicating endogenous peroxidase activity with 3% H_2O_2 and blocking non-specific antigens with goat serum, the sections were subjected to incubation with specific antibodies (Additional file 1: Table S2). The section signals were measured using DAB substrate (Maixin Biotech. Corporation, Fuzhou, China), and staining intensities were evaluated as previously described [23].

Bioinformatics analysis

Bioinformatics analysis was carried out as described in our previous study [24]. The mRNA-Seq (HTSeq-FPKM) and genomic data from the cervical squamous cell carcinoma and endocervical adenocarcinoma (CESC) dataset in The Cancer Genome Atlas (TCGA) database, together with clinical data were used to perform differential expression analysis with the limma R package, and correlation analysis, survival analysis, gene set enrichment analysis (GSEA), gene set variation analysis (GSVA), and unsupervised PAM clustering analyses with the ConsensusClusterPlus R package [25]. The Maftools R package was used for defining mutation co-occurrence/mutually exclusive. The platinum drug resistance- and the radioresistance-associated gene sets were established based on KEGG websites and a previous study [26], respectively. Samples were classified into high and low expression groups according to the best cut-off value for survival analysis in TCGA database.

Statistical analysis

The continuous variables are calculated as the mean \pm SD from at least three independent experiments and categorical variables are expressed as n (%). The data were analyzed using SPSS 22.0 or RStudio. A parametric generalized linear model with random effects for the growth curve, the Student's two-tailed t -test, and the Wilcoxon rank-sum tests for two groups, and one-way ANOVA with LSD- t test for multiple groups were used for detecting statistical significance. The correlation analyses were performed using the chi-square and Spearman's rank correlation tests. Kaplan–Meier survival curves were plotted and log-rank tests were applied for exploring a survival difference. Cox regression models were adopted to identify the relationship between CENPK and the survival time of cervical cancer patients. All statistical tests were

two-sided and a P value < 0.05 was considered statistically significant.

Results

Bioinformatics analyses revealed the involvement of m⁶A modification in cervical cancer progression

To better understand whether and how m⁶A regulators contribute to cervical cancer progression, we first identified 9 m⁶A writers (*WTAP*, *ZC3H13*, *METTL3*, *METTL14*, *METTL16*, *VIRMA*, *RBM15B*, *RBM15*, and *CBL1*), 15 m⁶A readers (*FMRI*, *hmRNPA2B1*, *hmRNPC*, *YTHDF1/2/3*, *YTHDC1/2*, *LRPPRC*, *IGF2BP1*, *IGF2BP2*, *IGF2BP3*, *RBMX*, *EIF3A*, and *ELAVL1*), and 2 m⁶A erasers (*FTO* and *ALKBH5*) that were previously reported to have pathogenic roles in other human cancer types [7, 8]. Using the TCGA CESC database, we identified copy number variations (CNVs) and somatic mutations in the m⁶A-related genes because amplification or deletions that affect copy number can also affect expression of the corresponding gene. This analysis showed that 21 m⁶A regulators harbored CNVs in cervical cancer (Additional file 2: Fig. S1). Among these genes, 13 of the 21 carried mutations at a frequency of 1–4%, while the remaining 8 genes had mutations at a frequency of $< 1\%$ (Additional file 2: Fig. S2a). Analysis of mutation co-occurrence indicated that several of these genes also carried mutations that significantly co-occurred with mutations in other m⁶A regulators (Additional file 2: Fig. S2b). RNA-seq data in the TCGA database further showed that these m⁶A regulators were differentially expressed in cervical cancer samples compared with the expression in adjacent normal tissues (Additional file 2: Fig. S2c), which suggested that CNVs and other somatic mutations could lead to dysregulation of the m⁶A-related genes in cervical cancer.

Continuing our analysis of possible relationships between m⁶A-related genes and cervical cancer in public datasets, we next focused on the potential clinical significance of these genes. Survival analyses indicated that 15 CNV-carrying genes had altered levels of expression that were significantly correlated with cervical cancer patient prognosis (Additional file 2: Fig. S3), whereas 6 of the genes showed no significant value as candidate prognostic indicators. Subsequent gene interaction network analysis indicated that 3 genes (*ZC3H13*, *METTL14*, and *CBL1*) appeared to serve as network hubs, suggesting that dysregulation of m⁶A modification by these genes provided major contributions to the development and/or progression of cervical cancer (Additional file 2: Fig. S4a). Correlation analyses also revealed a strong association among these 21 m⁶A regulators (Additional file 2: Fig. S4b). Notably, unsupervised clustering of the 21 m⁶A-related gene expression patterns in different

patients identified three distinct patterns of m⁶A modification (i.e., clusters A-C) associated with cervical cancer (Additional file 2: Fig. S4c, d). Survival analyses showed that the prognosis of patients with cluster B pattern generally had a better prognosis than patients exhibiting cluster A or C patterns (Additional file 2: Fig. S4e).

To determine the biological significance of these m⁶A modification patterns, we conducted GSVA to elucidate differentially-enriched KEGG pathways and GO terms in these clusters that are related to the m⁶A modification patterns identified in cervical cancer samples. The results showed that clusters A and C were enriched for canonical cancer signaling pathways and processes, such as the VEGF, mTOR, ERBB, MAPK, Wnt, TGF- β , hedgehog, and Notch pathways, as well as tight junctions, adherens junctions, cell cycle, non-homologous end joining, mitotic sister chromatid cohesion, mRNA processing, and related GO terms compared with samples exhibiting cluster B patterns (Additional file 2: Fig. S5), further indicating the involvement of m⁶A modification in cervical cancer progression.

CENPK expression is correlated with aberrant m⁶A modification and tumorigenic gene expression in cervical cancer

We compared the differential expression data from these 21 genes with the m⁶A methylation data available in the m⁶A-Atlas database and the data obtained in our previous study of cervical cancer patients [23] to identify specific genes that could be dysregulated by m⁶A modification in cervical cancer. First, we performed differential expression analyses between m⁶A cluster B and C patterns, which identified 3628 differentially-expressed genes in different m⁶A clusters [fold-change \geq 2.0 (geneset A); $P < 0.05$]. Furthermore, experimental evidence in the m⁶A-Atlas database (<http://180.208.58.66/m6A-Atlas/>) suggested the participation of 7617 genes with an m⁶A modification in HeLa cells (geneset B). Our previous study [23] also showed a possible correlation between 151 differentially-expressed genes and cervical cancer cell progression [fold-change \geq 2.0 (geneset C); $P < 0.05$]. A total of 40 overlapping genes were obtained from the intersection of the 3 genesets (Additional file 2: Fig. S6a).

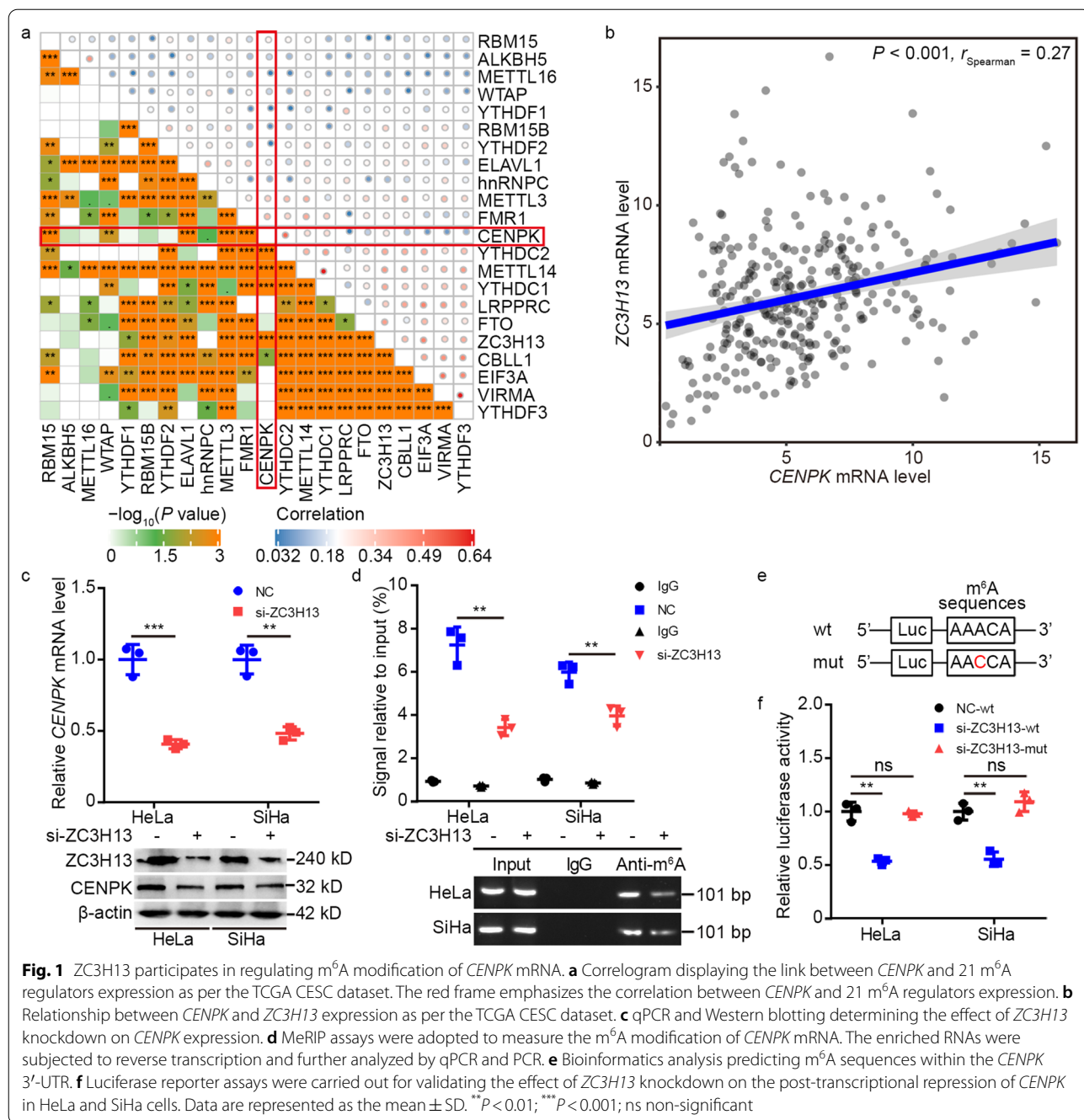
Subsequent GSVA revealed that pathways involving *CENPK* had the greatest overlap with m⁶A-modified clusters associated with cervical cancer. Specifically, *CENPK* was enriched for genes in pathways, such as Wnt signaling, DNA damage repair signaling, the cell cycle, and DNA replication (Additional file 2: Fig. S6b). *CENPK* expression was elevated in pan-cancer datasets compared to that in corresponding normal tissues based on TCGA (Additional file 2: Fig. S6c). Interestingly, GSEA showed that *CENPK* also participated in the modulation

of platinum drug resistance more prominently than radioresistance (Additional file 2: Fig. S6d). In addition, correlation analyses showed a positive association between *CENPK* and stemness markers, including *EPCAM*, *CD133*, *SOX2*, and *OCT4* (Additional file 2: Fig. S6e). Taken together, these results indicated a strong correlation between *CENPK* expression and the dysregulation of m⁶A modifications in cervical cancer.

ZC3H13-mediated m⁶A methylation upregulated CENPK mRNA to activate pro-tumorigenic functions

We further examined whether *CENPK* expression was regulated by m⁶A RNA methylation based on the results of our bioinformatics analyses. The above mentioned survival analysis showed 9 m⁶A regulators (*EIF3A*, *hmRNPC*, *LRPPRC*, *RBM15B*, *VIRMA*, *WTAP*, *YTHDF2*, *YTHDF3*, and *ZC3H13*) with the potential to confer poor patient survival (Additional file 2: Fig. S3). Indeed, *CENPK* expression was correlated with *CBL1*, *ELAVL1*, *FMRI*, *METTL3*, *METTL14*, *RBM15*, *WTAP*, *YTHDC1*, *YTHDC2*, and *ZC3H13* expression (Fig. 1a, b). Thus, *ZC3H13* and *WTAP* were correlated with poor patient survival and *CENPK* expression, and of these two candidates, *CENPK* had a more prominent correlation with *ZC3H13* expression than with *WTAP* expression. Because *CENPK* has a potential oncogenic role in cervical cancer, we speculated that *ZC3H13* might be responsible for m⁶A methylation of *CENPK* mRNA. To test this possibility, we generated HeLa and SiHa cells with *ZC3H13* knockdown by siRNA (si-ZC3H13), which downregulated *CENPK* expression (Fig. 1c). In addition, MeRIP assays confirmed that *CENPK* mRNA was enriched by anti-m⁶A antibody in HeLa and SiHa cells, while m⁶A modification of *CENPK* mRNA was reduced in si-ZC3H13 cells (Fig. 1d). Moreover, DART-seq data in the RMVar database (<http://rmvar.renlab.org>) identified a site in the 3' UTR of *CENPK* mRNA on chr5:65518395(-) as an m⁶A modification site (Fig. 1e). Luciferase reporter assays suggested that even though *ZC3H13* suppression impaired the transcription of wild-type *CENPK*, non-synonymous cytosine-to-adenosine conversion mutations at this m⁶A site abolished the downregulation (Fig. 1f). These results thus indicated that *CENPK* expression was modulated by *ZC3H13*-associated m⁶A modification.

Based on these findings, we further investigated the effects of *ZC3H13* on *CENPK*-mediated downstream signaling. Considering its overlap with cervical cancer-enriched pathways (vide supra), we focused on Wnt and p53 signaling. TOP/FOP luciferase reporter and dual-luciferase assays revealed that *ZC3H13* knockdown decreased Wnt signaling activity and elevated p53 signaling activity in HeLa and SiHa cells, but this effect was



abolished by overexpressing *CENPK* (ov-*CENPK*) (Additional file 2: Fig. S7a, b). Indeed, tumorsphere and colony formation, and Transwell, EdU, and immunofluorescence staining assays showed that *ZC3H13* knockdown had a suppressive effect on cervical cancer stemness, chemoresistance, metastasis, and cell proliferation that was reversed by ov-*CENPK* in HeLa and SiHa cells (Additional file 2: Fig. S7c-i). These results collectively demonstrated that *ZC3H13* functioned as a regulator of *CENPK*

expression through m⁶A RNA methylation and that these genes functioned together in facilitating cervical cancer progression.

CENPK expression was correlated with cervical cancer pathology

To further establish the central role of *CENPK* in cervical cancer, we conducted IHC analysis of 119 cervical cancer samples and 35 adjacent normal tissues. The results

showed elevation of CENPK expression in cervical cancer compared with adjacent normal tissues (Fig. 2a). Moreover, IHC staining of CENPK protein indicated a positive association with Ki67 protein levels (Fig. 2b) and was positively correlated with cancer recurrence (Additional file 1: Table S3).

Survival analysis suggested that cervical cancer patients with high CENPK expression exhibited poor overall survival (Fig. 2c). Because CENPK expression was correlated with cancer recurrence, we further investigated the relationship between CENPK expression and recurrence-free survival in cervical cancer patients. Survival analysis of cervical cancer patients confirmed that high CENPK expression was a predictor of poor recurrence-free survival, which is consistent with correlation analysis (Fig. 2d). Quantitative analysis of IHC staining, followed by univariate and multivariate COX hazard analyses, indicated that CENPK expression was an independent and unfavorable prognostic indicator for overall and recurrence-free survival in cervical cancer patients (Fig. 2e, f). A nomogram showing the role of CENPK, age, and T classification in predicting cancer recurrence in cervical cancer patients is shown in Fig. 2g. When stratified by age or T classification, CENPK expression remained correlated with overall and recurrence-free survival (Additional file 2: Fig. S8a, b). Consistent with these results, correlation analyses suggested a positive association between β -catenin, Ki67, and CENPK expression (Additional file 2: Fig. S8c). Moreover, ZC3H13 expression was positively associated with EPCAM, CD133, β -catenin, Ki67, N-cadherin, and CCND1 expression in the TCGA database (Additional file 2: Fig. S8d). Taken together, these data showed a clear role for CENPK in cervical cancer development and indicated the clinical value as a potential biomarker.

Silencing CENPK suppressed cervical cancer stemness, chemoresistance, metastasis, and proliferation

Given this validation of CENPK contribution to cervical cancer, we sought to determine how CENPK affected cell stemness, chemoresistance, metastasis, and proliferation. To this end, CENPK was silenced by shRNA (sh-CENPK) or siRNA (si-CENPK) in HeLa and SiHa cell lines. Tumorsphere formation assays and immunofluorescence staining of cervical cancer stem cell markers (CD133 and CD44) indicated that CENPK knockdown reduced stemness of HeLa and SiHa cells (Fig. 3a, b). Clonogenic assays revealed that CENPK suppression impaired cisplatin and carboplatin resistance (Fig. 3c), Transwell assays showed impaired migration and invasion (Fig. 3d), and MTT and colony formation assays revealed inhibited cell growth by sh-CENPK or si-CENPK in HeLa and SiHa cells (Fig. 3e, f). Moreover, immunofluorescence staining

of γ -H2AX (Ser139) showed that downregulation of CENPK led to enhanced DNA damage in cervical cancer cells treated with platinum-based drugs (Fig. 3g). Consistent with the bioinformatics results, EdU assays suggested that CENPK knockdown decreased the percentage of cells in the S phase and inhibited DNA replication in HeLa and SiHa cells (Fig. 3h). In addition, the expression of DNA damage repair-associated proteins (p53 and p21) was enhanced, while cell stemness, epithelial-mesenchymal transition (EMT), and DNA replication-associated proteins (c-Myc, Vimentin, CCND1, and c-Jun) were suppressed in si-CENPK cells (Fig. 3i; Additional file 2: Fig. S9). These results indicated that high CENPK expression stimulated cervical cancer stemness, chemoresistance, metastasis, and proliferation.

We established cervical cancer models in BALB/c-nu mice harboring wild-type or stably-silenced CENPK to determine how CENPK affected cancer progression in vivo. We confirmed that CENPK expression was decreased in tumors treated with CENPK-targeted shRNA (Fig. 4a). Mice with downregulated CENPK in HeLa and SiHa cells exhibited decreased tumor formation, fewer lung metastases, and slower growth rates than the corresponding controls (Fig. 4b-f). IHC staining also showed lower Ki67 expression in sh-CENPK tumors compared to scramble shRNA control tumors (Fig. 4g). Moreover, CENPK silencing prolonged the overall survival time of model mice, and CENPK suppression led to synergistic effects with chemotherapy to further extend the mouse survival time compared with that of mice receiving chemotherapy only (Fig. 4h).

CENPK activated Wnt signaling and inactivated p53 signaling via SOX6 in cervical cancer

We next determined the specific mechanisms by which CENPK exerted oncogenic effects. A review of the BioGRID database (<https://downloads.thebiogrid.org/BioGRID>) suggested that SOX6 potentially interacted with CENPK, and our above bioinformatics analysis indicated that CENPK modulated Wnt signaling (Additional file 2: Fig. S6). Together with TOP/FOP-flash assays, which confirmed CENPK promoted Wnt signaling (Fig. 5a), and previous studies that showed SOX6 activated p53 signaling and inactivated Wnt signaling [27] while also suppressing cervical cancer progression [28], we selected SOX6 as a candidate protein interaction partner of CENPK. Co-IP assays verified that CENPK interacted with SOX6 (Fig. 5b), and immunofluorescent staining confirmed the co-localization of CENPK and SOX6 in HeLa and SiHa cells (Fig. 5c).

SOX6 is known to inhibit the transcription of target genes regulated by β -catenin via direct interaction with β -catenin to inactivate Wnt signaling [27]. Moreover,

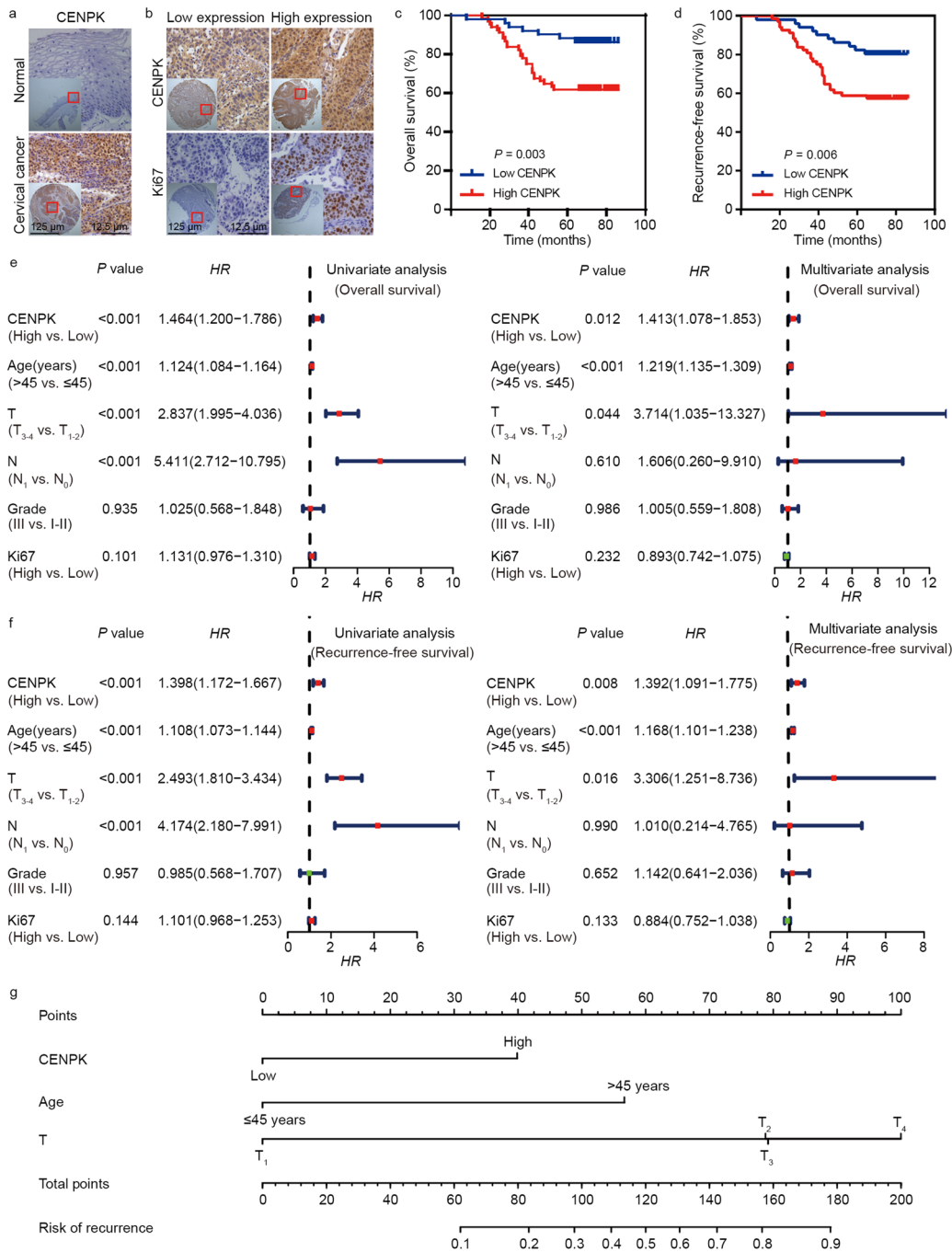


Fig. 2 CENPK expression is elevated in cervical cancer and confers poor patient prognosis. **a** Representative images showing the differential CENPK expression between cervical cancer and adjacent normal tissues. **b** Representative images showing the relationship between CENPK and Ki67 expression in cervical cancer. **c** Kaplan–Meier survival analysis disclosing the overall survival of cervical cancer patients according to CENPK expression. **d** Kaplan–Meier survival analysis displaying the recurrence-free survival of cervical cancer patients according to CENPK expression. **e** Univariate and multivariate analyses were adopted for correlating CENPK expression, clinicopathological characteristics, and overall survival of cervical cancer patients. **f** Univariate and multivariate analyses were performed to correlate CENPK expression, clinicopathological characteristics, and recurrence-free survival of cervical cancer patients. **g** Development of a nomogram for predicting cancer recurrence of cervical cancer patients. HR hazard ratio

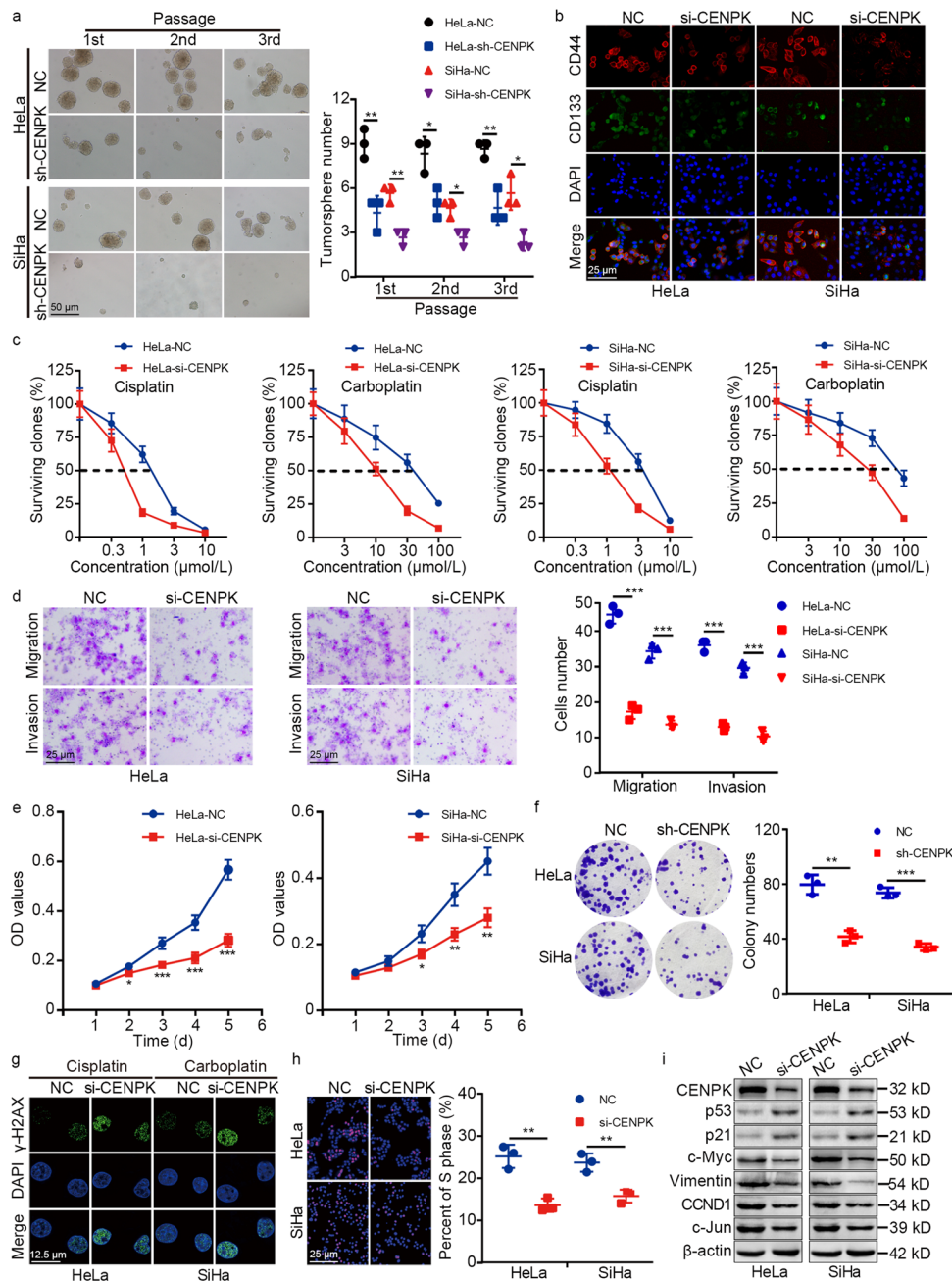


Fig. 3 CENPK promotes cervical cancer stemness, chemoresistance, metastasis, and proliferation. Tumorsphere formation (a) and immunofluorescence assays (b) were adopted to measure stemness of *CENPK*-depleted HeLa and SiHa cells and the control cells. c Clonogenic assays were adopted to estimate chemoresistance of *CENPK*-depleted HeLa and SiHa cells and the control cells treated with cisplatin and carboplatin. d Transwell assays were performed to elucidate the migration and invasion of *CENPK*-silenced HeLa and SiHa cells and the control cells. MTT assays (e), and colony-formation assays (f) were applied to evaluate the proliferation of *CENPK*-silenced HeLa and SiHa cells and the control cells. g Immunofluorescence was adopted for detecting the expression of γ-H2AX (Ser139) in *CENPK*-silenced HeLa treated with cisplatin (10 μmol/L for 24 h), *CENPK*-silenced SiHa cells treated with carboplatin (100 μmol/L for 24 h), and control cells. h EdU incorporation assays were used for elucidating DNA replication of *CENPK*-depleted HeLa and SiHa cells and the control cells. i Western blotting analysis of the expression of proteins associated with stemness (c-Myc), DNA damage repair (p53), epithelial-mesenchymal transition (Vimentin), and DNA replication (p21, CCND1 and c-Jun) in *CENPK*-depleted HeLa and SiHa cells and control cells. Data are represented as the mean ± SD. **P* < 0.05, ***P* < 0.01, ****P* < 0.001

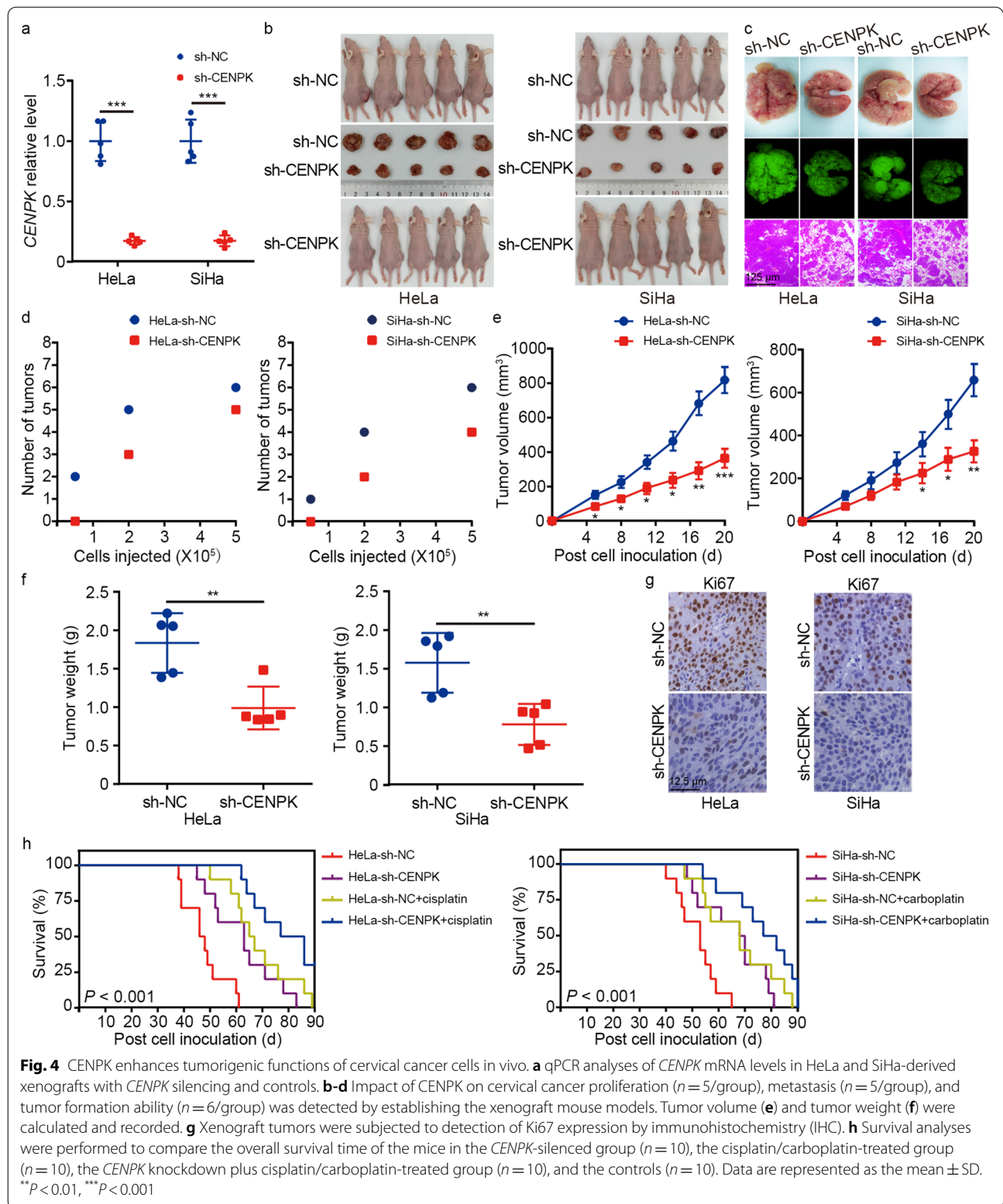
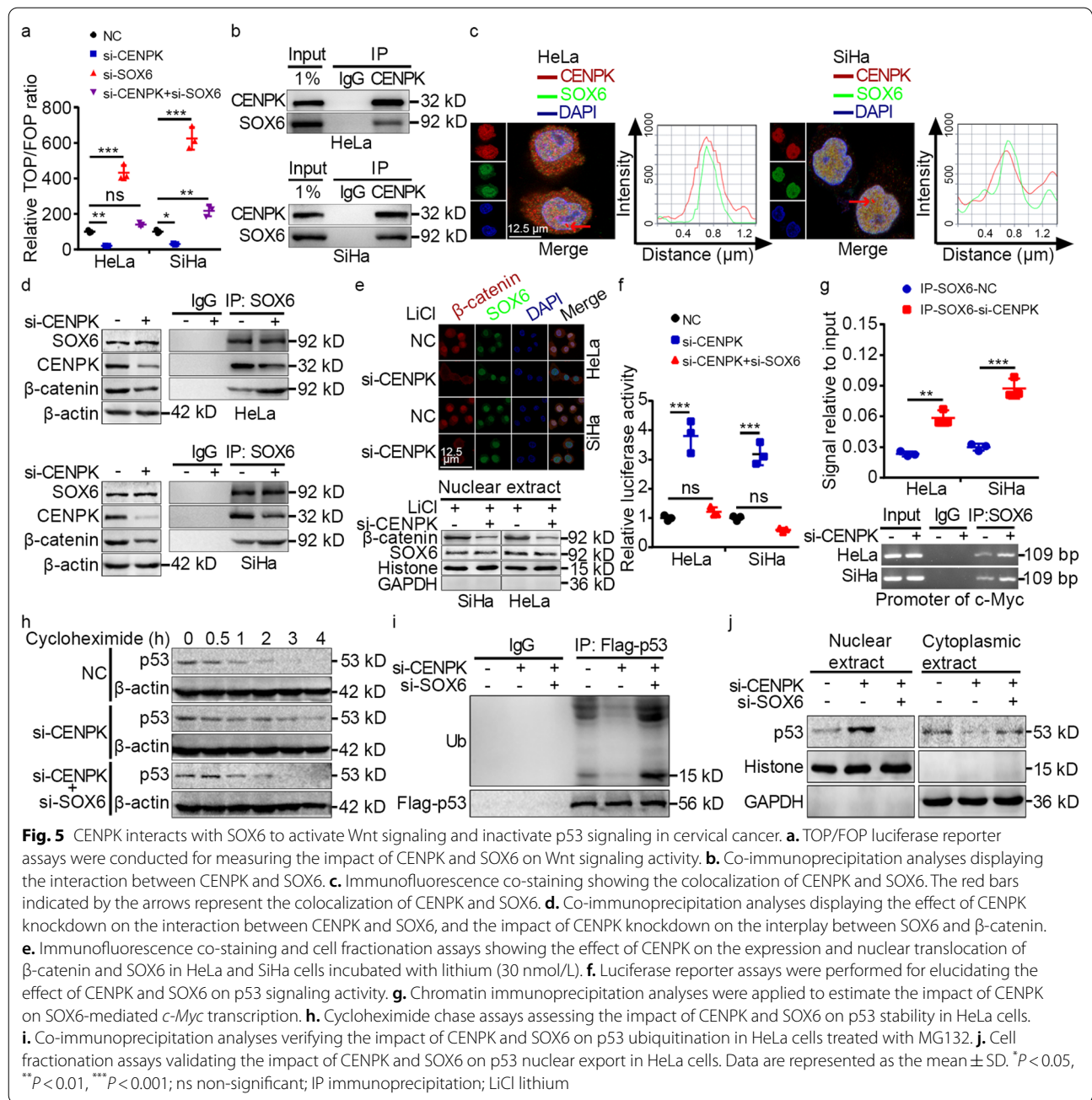


Fig. 4 CENPK enhances tumorigenic functions of cervical cancer cells in vivo. **a** qPCR analyses of *CENPK* mRNA levels in HeLa and SiHa-derived xenografts with *CENPK* silencing and controls. **b-d** Impact of CENPK on cervical cancer proliferation ($n = 5/\text{group}$), metastasis ($n = 5/\text{group}$), and tumor formation ability ($n = 6/\text{group}$) was detected by establishing the xenograft mouse models. Tumor volume (**e**) and tumor weight (**f**) were calculated and recorded. **g** Xenograft tumors were subjected to detection of Ki67 expression by immunohistochemistry (IHC). **h** Survival analyses were performed to compare the overall survival time of the mice in the *CENPK*-silenced group ($n = 10$), the cisplatin/carboplatin-treated group ($n = 10$), the *CENPK* knockdown plus cisplatin/carboplatin-treated group ($n = 10$), and the controls ($n = 10$). Data are represented as the mean \pm SD. ** $P < 0.01$, *** $P < 0.001$



TOP/FOP-flash assays suggested that SOX6 knockdown had regulatory functions in CENPK-mediated Wnt signaling (Fig. 5a). These results thus implied that CENPK-SOX6 interaction might affect interactions between SOX6 and β -catenin. Co-IP analyses subsequently revealed an interaction between SOX6 and β -catenin, and this SOX6 interaction with β -catenin was enhanced in si-CENPK cells with decreased CENPK-SOX6 binding (Fig. 5d). Moreover, immunofluorescence staining and cell fractionation assays suggested that CENPK

knockdown inhibited β -catenin expression and nuclear translocation; however, no impact on SOX6 localization or expression by CENPK was detected (Fig. 5e).

We next investigated the effects of CENPK on p53 signaling in light of the report that SOX6 activates p53 signaling by increasing protein stability via transcriptional suppression of *c-Myc* in HeLa cells [28]. Dual-luciferase assays showed increased p53 signaling in CENPK knockdown cells, whereas SOX6 silencing abolished this effect (Fig. 5f). ChIP assays indicated that SOX6 binding to the

c-Myc transcription regulatory region was increased in HeLa and SiHa cells (Fig. 5g). Furthermore, cycloheximide chase assays, Co-IP analyses, and cell fractionation assays all confirmed that *CENPK* knockdown led to increased p53 stability and inhibition of p53 ubiquitination and nuclear export, all of which were reversed by *SOX6* knockdown (Fig. 5h-j). These data suggested that *SOX6* mediated the effects of *CENPK* on Wnt and p53 signaling.

CENPK promoted tumorigenic functions of cervical cancer cells via Wnt and p53 signaling

We then investigated how *CENPK* function in cervical cancer was mediated by Wnt and p53 signaling. Immunofluorescence staining, tumorsphere formation, clonogenic, MTT, and EdU assays collectively showed that *β-catenin* overexpression or *p53* knockdown reversed the inhibitory effects of *CENPK* knockdown on cell stemness, chemoresistance, migration, invasion, and proliferation in HeLa and SiHa cells (Additional file 2: Fig. S10a-f). Immunofluorescence staining and Western blotting further showed that *β-catenin* overexpression or *p53* knockdown abolished the diverse effects of *CENPK* knockdown on DNA damage repair, cell stemness, EMT, and DNA replication-associated gene expression [i.e., γ -H2AX (Ser139), p53, p21, *c-Myc*, Vimentin, *CCND1*, and *c-Jun*] (Additional file 2: Fig. S10g, h). These results thus showed that the pro-tumorigenic effects of *CENPK* were mediated by Wnt and p53 downstream regulatory targets.

Discussion

Stemness, chemoresistance, metastasis, and tumor size are known to contribute to cancer recurrence and poor prognosis in cervical cancer patients [29, 30]. Notably, m⁶A RNA methylation has been recently shown to play an important role in controlling biological processes required for the development and progression of human cancers, such as cell stemness, drug resistance, metastasis, and proliferation [31]. In the current study, we identified clear links between m⁶A RNA methylation and cervical cancer using bioinformatics analyses, thus suggesting that specific m⁶A modification patterns play a critical role in cervical cancer. Specifically, our work showed that m⁶A methylation regulated *CENPK* expression, and subsequently enhanced Wnt signaling and attenuated p53 signaling to modulate the expression of key regulators of DNA damage repair, EMT, and DNA replication. These downstream effects thus promoted the tumorigenic characteristics of cervical cancer cells, such as stemness, chemoresistance, metastasis, and proliferation. In contrast, *CENPK* downregulation resulted in delayed progression of cervical cancer in vitro and

in vivo. Moreover, high *CENPK* expression was positively correlated with poor overall and recurrence-free survival in cervical cancer patients.

Distinct m⁶A RNA methylation patterns have been shown to serve as determining factors in cancer immunity and patient prognosis [25]. Our bioinformatics analyses identified three m⁶A RNA methylation patterns associated with aberrant activity due to CNVs in 21 different m⁶A regulators. Because CNV affected the expression of these 21 m⁶A-related genes, it was reasonable to hypothesize that expression of the 21 m⁶A-related genes significantly contributed to cancer progression, as shown in our previous work [24]. The abnormal expression of these m⁶A-related genes and their prognostic value in cervical cancer further support the regulatory role of m⁶A RNA methylation in driving cancer development [25]. Based on the association between dysregulation of m⁶A methylation and cervical cancer, we were able to identify *CENPK* as a primary target of m⁶A RNA methylation that was also correlated with cancer development.

Previous studies have demonstrated that *ZC3H13* provided regulatory effects on stem cell self-renewal and oncogenesis of cervical cancer [32, 33]. Our findings further illustrated how *ZC3H13* functions in promoting the tumorigenic properties of cervical cancer cells via *CENPK*. Consistent with findings from a previous study that ablation of *ZC3H13* caused a global reduction of m⁶A modification, especially at the 3' ends of mRNA [34], we found that *CENPK* expression was modulated by *ZC3H13*-associated m⁶A modification in the 3'-UTR of *CENPK* mRNA in the current study. Moreover, we confirmed that *ZC3H13* enhanced *CENPK* expression, supporting the bioinformatic findings of m⁶A-mediated dysregulation of *CENPK* and the correlation between *ZC3H13* and *CENPK* in cervical cancer. Our results subsequently verified that *ZC3H13* was responsible for *CENPK* disturbance of Wnt and p53 signaling, suggesting that these genes function in concert to drive cervical cancer progression. Considering the global effects of *ZC3H13* on m⁶A modification, we noticed that the proposed Wnt and p53 signaling may not be the only axis responsible for *ZC3H13*-mediated cervical cancer progression.

In contrast, *SOX6* is known to function in tumor suppression of several cancers [35–37], including cervical cancer [38]. Moreover, *SOX6* has been shown to inhibit Wnt/ β -catenin signaling, but activate p53 signaling [39, 40]. Here, we demonstrated that *CENPK* interacted with *SOX6* to impair interactions between *SOX6* and β -catenin, as well as *SOX6*-mediated suppression of *c-Myc* transcription, which resulted in activating the Wnt signaling pathway and inactivating the p53 pathway. In addition, the positive regulation of β -catenin expression

by CENPK and its subsequent nuclear translocation contributed to Wnt pathway activation, which is consistent with findings reported in previous studies [21, 41]. Although p53 has been shown to positively regulate cancer cell resistance to platinum [42], Wnt signaling could also potentially mediate cancer cell resistance to platinum through several mechanisms, such as regulation of cancer stemness, EMT, and DNA damage repair [16, 43]. In addition, both the Wnt and p53 pathways have been shown to participate in regulating cancer cell stemness, metastasis, and proliferation [22, 44]. In our investigation, we further linked the dysregulation of these pathways with cervical cancer progression through the effects of CENPK in enhancing stemness, DNA damage repair (i.e., cisplatin and carboplatin resistance), EMT (necessary for tumor metastasis), and DNA replication processes related to cell proliferation. It should be noted, however, that our investigation using clinical samples was a single-center study, and the side effect of *CENPK* knockdown on the normal tissues was undetermined. Conducting a large-scale and multi-center study and constructing *CENPK* knockout mice to explore the possible impact caused by *CENPK* loss might overcome the limitations of our work.

Conclusions

Overall, the present study revealed a novel ZC3H13-CENPK-SOX6-p53/Wnt regulatory axis in cervical cancer development and progression through activation of tumorigenic functions, leading from m⁶A regulation of RNA. Furthermore, this work identified a previously unrecognized mechanism by which CENPK interfered with the interaction between SOX6 and β -catenin by direct binding with SOX6. This disruption of SOX6 activity resulted in increased β -catenin expression and nuclear translocation, and enhanced p53 ubiquitination and nuclear export, thereby upregulating Wnt signaling and downregulating p53 signaling. Finally, our results indicated that the m⁶A regulator (ZC3H13) was responsible for stimulating CENPK/SOX6 activation of Wnt/ β -catenin and suppression of the p53 axis in this regulatory axis for cervical cancer progression (Fig. 6). This work thus demonstrated a role for m⁶A RNA methylation in controlling specific signaling pathways and highlighted a theoretic framework for clinical application of CENPK as a prognostic indicator and as a novel target for cervical cancer treatments.

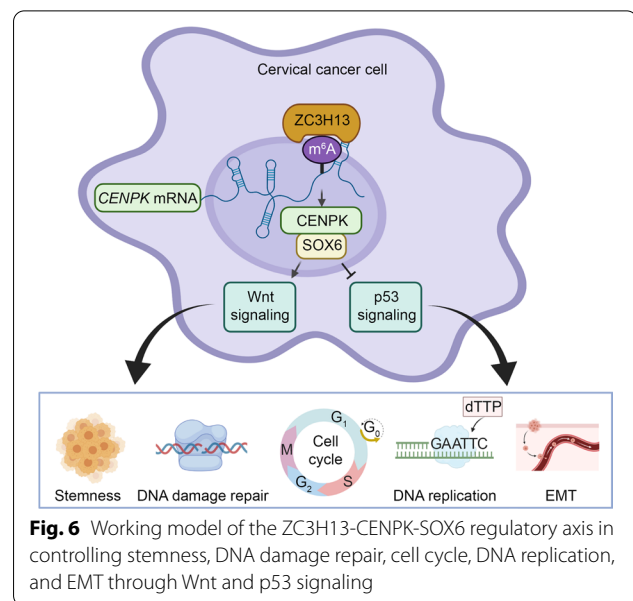


Fig. 6 Working model of the ZC3H13-CENPK-SOX6 regulatory axis in controlling stemness, DNA damage repair, cell cycle, DNA replication, and EMT through Wnt and p53 signaling

Abbreviations

CENPK: Centromere protein K; CESC: Cervical squamous cell carcinoma and endocervical adenocarcinoma; ChIP: Chromatin immunoprecipitation; CI: Confidence interval; CNVs: Copy number variations; Co-IP: Co-immunoprecipitation; DMEM: Dulbecco's modified Eagle medium; EMT: Epithelial-mesenchymal transition; GSEA: Gene set enrichment analysis; GSVA: Gene set variation analysis; HR: Hazard ratio; IHC: Immunohistochemistry; MeRIP: Methylated RNA Immunoprecipitation; m⁶A: N⁶-Methyladenine; qPCR: Quantitative real-time PCR; RT-PCR: Reverse transcription-polymerase chain reaction; TCGA: The Cancer Genome Atlas.

Supplementary Information

The online version contains supplementary material available at <https://doi.org/10.1186/s40779-022-00378-z>.

Additional file 1. Table S1 Sequences used in this study. **Table S2** A list of antibodies used for ChIP, Co-IP, IF, IHC, and WB. **Table S3** Correlation between CENPK expression and the clinicopathological characteristics of cervical cancer patients.

Additional file 2. Fig. S1 DNA copy number variation of 21 m⁶A regulators in cervical cancer based on TCGA database. **Fig. S2** Genetic and expression variation profiles of m⁶A regulators in cervical cancer based on TCGA database. **Fig. S3** Survival analysis of cervical patients in TCGA database. **Fig. S4** Unsupervised clustering of m⁶A regulators as per TCGA CESC dataset. **Fig. S5** Gene set variation analysis identifies the involvement of biological characteristics in distinct m⁶A methylation patterns. **Fig. S6** Bioinformatics analyses of m⁶A-modified *CENPK* based on the microarray and TCGA data. **Fig. S7** ZC3H13 augments pro-tumorigenic functions of cervical cancer cells through CENPK-modulated Wnt and p53 signaling. **Fig. S8** CENPK confers poor patient prognosis by stratified analysis and its relationship with related genes expression. **Fig. S9** CENPK promotes cervical cancer stemness, chemoresistance, metastasis, and proliferation. **Fig. S10** CENPK augments pro-tumorigenic functions of cervical cancer cells through Wnt and p53 signaling.

Acknowledgements

The authors sincerely compliment the staff of the pathology department for completing the project.

Author contributions

QX and CC conceived and designed this study. XL, FW, and JC performed the experiments and prepared the manuscript; XL, FW, JC, JL, YBL, and LL conducted the data analyses. All authors read manuscript drafts, contributed edits, and approved the final manuscript.

Funding

This study was supported by the Joint Funds for the Innovation of Science and Technology Program of Fujian Province, China (2018Y9110), the Natural Science Foundation of Fujian Province, China, (2020J011126), and the China Postdoctoral Science Foundation (2021T140468).

Declarations

Ethics approval and consent to participate

Patient consent and ethics approval were obtained from the Ethics Committee of Shanghai Outdo Biotech Corporation (YB M-05-02). The procedures used in this study adhere to the tenets of the Declaration of Helsinki. The Institutional Animal Ethical Committee, Experimental Animal Center of Fujian Medical University and Fujian Cancer Hospital approved the protocols for animal studies (K2020-036-01).

Consent for publication

Not applicable.

Availability of data and materials

The datasets used and/or analyzed during the current study are available from the corresponding author on reasonable request.

Competing interests

The authors declare that they have no competing interests.

Author details

¹Departments of Gynecology, Fujian Cancer Hospital and Fujian Medical University Cancer Hospital, Fujian Medical University, Fuzhou 350014, China. ²Department of Radiation Oncology, Fujian Cancer Hospital and Fujian Medical University Cancer Hospital, Fujian Medical University, Fuzhou 350014, China. ³Shenzhen Key Laboratory of Immunity and Inflammatory Diseases, Peking University Shenzhen Hospital, Shenzhen Peking University-the Hong Kong University of Science and Technology Medical Center, Shenzhen 518036, Guangdong, China. ⁴Outpatient Department, Fujian Hospital of People's Armed Police, Fujian Medical University, Fuzhou 350014, China.

Received: 17 December 2021 Accepted: 1 April 2022

Published online: 14 April 2022

References

- Sung H, Ferlay J, Siegel RL. Global cancer statistics 2020: GLOBOCAN estimates of incidence and mortality worldwide for 36 cancers in 185 countries. *CA Cancer J Clin*. 2021;71(3):209–49.
- Siegel RL, Miller KD, Fuchs HE, Jemal A. Cancer statistics, 2021. *CA Cancer J Clin*. 2021;71(1):7–33.
- He Y, Xiao M, Fu H, Chen L, Qi L, Liu D, et al. cPLA2 α reversibly regulates different subsets of cancer stem cells transformation in cervical cancer. *Stem Cells*. 2020;38(4):487–503.
- Wang H, Luo Q, Kang J, Wei Q, Yang Y, Yang D, et al. YTHDF1 aggravates the progression of cervical cancer through m⁶A-Mediated up-regulation of RANBP2. *Front Oncol*. 2021;11:650383.
- Li Z, Peng Y, Li J, Chen Z, Chen F, Tu J, et al. N⁶-methyladenosine regulates glycolysis of cancer cells through PDK4. *Nat Commun*. 2020;11(1):2578.
- Wang Q, Guo X, Li L, Gao Z, Su X, Ji M, et al. N⁶-methyladenosine METTL3 promotes cervical cancer tumorigenesis and Warburg effect through YTHDF1/HK2 modification. *Cell Death Dis*. 2020;11(10):911.
- Zhao H, Xu Y, Xie Y, Zhang L, Gao M, Li S, et al. m⁶A regulators is differently expressed and correlated with immune response of esophageal cancer. *Front Cell Dev Biol*. 2021;9:650023.
- Zhao Y, Shi Y, Shen H, Xie W. m⁶A-binding proteins: the emerging crucial performers in epigenetics. *J Hematol Oncol*. 2020;13(1):35.
- Lee YC, Huang CC, Lin DY, Chang WC, Lee KH. Overexpression of centromere protein K (CENPK) in ovarian cancer is correlated with poor patient survival and associated with predictive and prognostic relevance. *PeerJ*. 2015;3:e1386.
- Komatsu M, Yoshimaru T, Matsuo T, Kiyotani K, Miyoshi Y, Tanahashi T, et al. Molecular features of triple negative breast cancer cells by genome-wide gene expression profiling analysis. *Int J Oncol*. 2013;42(2):478–506.
- Wang H, Liu W, Liu L, Wu C, Wu W, Zheng J, et al. Overexpression of centromere protein K (CENP-K) gene in hepatocellular carcinoma promote cell proliferation by activating AKT/TP53 signal pathway. *Oncotarget*. 2017;8(43):73994–4005.
- Liu Y, Xiong S, Liu S, Chen J, Yang H, Liu G, et al. Analysis of gene expression in bladder cancer: possible involvement of mitosis and complement and coagulation cascades signaling pathway. *J Comput Biol*. 2020;27(6):987–98.
- Liu Y, Hu H, Zhang C, Wang H, Zhang W, Wang Z, et al. Co-expression of mitosis-regulating genes contributes to malignant progression and prognosis in oligodendrogliomas. *Oncotarget*. 2015;6(35):38257–69.
- Ma J, Chen X, Lin M, Wang Z, Wu Y, Li J. Bioinformatics analysis combined with experiments predicts CENPK as a potential prognostic factor for lung adenocarcinoma. *Cancer Cell Int*. 2021;21(1):65.
- Okada M, Cheeseman IM, Hori T, Okawa K, McLeod IX, Yates JRR, et al. The CENP-H complex is required for the efficient incorporation of newly synthesized CENP-A into centromeres. *Nat Cell Biol*. 2006;8(5):446–57.
- Zou Y, Lin X, Bu J, Lin Z, Chen Y, Qiu Y, et al. Timeless-stimulated miR-5188-FOXO1/ β -catenin-c-Jun feedback loop promotes stemness via ubiquitination of β -catenin in breast cancer. *Mol Ther*. 2020;28(1):313–27.
- Koivusalo R, Krausz E, Ruotsalainen P, Helenius H, Hietanen S. Chemoradiation of cervical cancer cells: targeting human papillomavirus E6 and p53 leads to either augmented or attenuated apoptosis depending on the platinum carrier ligand. *Cancer Res*. 2002;62(24):7364–71.
- Zhou F, Yang X, Zhao H, Liu Y, Feng Y, An R, et al. Down-regulation of OGT promotes cisplatin resistance by inducing autophagy in ovarian cancer. *Theranostics*. 2018;8(19):5200–12.
- Segovia-Mendoza M, Jurado R, Mir R, Medina LA, Prado-Garcia H, Garcia-Lopez P. Antihormonal agents as a strategy to improve the effect of chemo-radiation in cervical cancer: in vitro and in vivo study. *BMC Cancer*. 2015;15:21.
- Mukherjee A, Chiang CY, Daifotis HA. Adipocyte-induced FABP4 expression in ovarian cancer cells promotes metastasis and mediates carboplatin resistance. *Cancer Res*. 2020;80(8):1748–61.
- Lin X, Zuo S, Luo R, Li Y, Yu G, Zou Y, et al. HBx-induced miR-5188 impairs FOXO1 to stimulate β -catenin nuclear translocation and promotes tumor stemness in hepatocellular carcinoma. *Theranostics*. 2019;9(25):7583–98.
- Lin X, Li AM, Li YH, Luo RC, Zou YJ, Liu YY, et al. Silencing MYH9 blocks HBx-induced GSK3 β ubiquitination and degradation to inhibit tumor stemness in hepatocellular carcinoma. *Signal Transduct Target Ther*. 2020;5(1):13.
- Xu Q, Chen C, Liu B, Lin Y, Zheng P, Zhou D, et al. Association of iRhom1 and iRhom2 expression with prognosis in patients with cervical cancer and possible signaling pathways. *Oncol Rep*. 2020;43(1):41–54.
- Lin X, Zheng X, Yang B, Chen J, Xu Q, Wang Q. Clinical significance and immune landscapes of stemness-related and immune gene set-based signature in oral cancer. *Clin Transl Med*. 2021;11(2):e343.
- Zhang B, Wu Q, Li B, Wang D, Wang L, Zhou YL. m⁶A regulator-mediated methylation modification patterns and tumor microenvironment infiltration characterization in gastric cancer. *Mol Cancer*. 2020;19(1):53.
- Kitahara O, Katagiri T, Tsunoda T, Harima Y, Nakamura Y. Classification of sensitivity or resistance of cervical cancers to ionizing radiation according to expression profiles of 62 genes selected by cDNA microarray analysis. *Neoplasia*. 2002;4(4):295–303.
- Dong P, Xiong Y, Yu J, Chen L, Tao T, Yi S, et al. Control of PD-L1 expression by miR-140/142/340/383 and oncogenic activation of the OCT4-miR-18a pathway in cervical cancer. *Oncogene*. 2018;37(39):5257–68.

28. Wang J, Ding S, Duan Z, Xie Q, Zhang T, Zhang X, et al. Role of p14ARF-HDM2-p53 axis in SOX6-mediated tumor suppression. *Oncogene*. 2016;35(13):1692–702.
29. Budhwani M, Lukowski SW, Porceddu SV, Frazer IH, Chandra J. Dysregulation of stemness pathways in HPV mediated cervical malignant transformation identifies potential oncotherapy targets. *Front Cell Infect Microbiol*. 2020;10:307.
30. Lee SW, Lee SH, Kim J, Kim YS, Yoon MS, Jeong S, et al. Magnetic resonance imaging during definitive chemoradiotherapy can predict tumor recurrence and patient survival in locally advanced cervical cancer: a multi-institutional retrospective analysis of KROG 16–01. *Gynecol Oncol*. 2017;147(2):334–9.
31. Li B, Jiang J, Assaraf YG, Xiao H, Chen ZS, Huang C. Surmounting cancer drug resistance: new insights from the perspective of N⁶-methyladenosine RNA modification. *Drug Resist Updat*. 2020;53:100720.
32. Wen J, Lv R, Ma H, Shen H, He C, Wang J, et al. Zc3h13 regulates nuclear RNA m⁶A methylation and mouse embryonic stem cell self-renewal. *Mol Cell*. 2018;69(6):1028–38.
33. Pan J, Xu L, Pan H. Development and validation of an m⁶A RNA methylation regulator-based signature for prognostic prediction in cervical squamous cell carcinoma. *Front Oncol*. 2020;10:1444.
34. Knuckles P, Lence T, Haussmann IU, Jacob D, Kreim N, Carl SH, et al. Zc3h13/Flacc is required for adenosine methylation by bridging the mRNA-binding factor Rbm15/Spenito to the m⁶A machinery component Wtap/Fl(2)d. *Genes Dev*. 2018;32(5–6):415–29.
35. Jiang W, Yuan Q, Jiang Y, Huang L, Chen C, Hu G, et al. Identification of Sox6 as a regulator of pancreatic cancer development. *J Cell Mol Med*. 2018;22(3):1864–72.
36. Liang Z, Xu J, Gu C. Novel role of the SRY-related high-mobility-group box D gene in cancer. *Semin Cancer Biol*. 2020;67(Pt 1):83–90.
37. Lin M, Lei T, Zheng J, Chen S, Du L, Xie H. UBE2S mediates tumor progression via SOX6/ β -Catenin signaling in endometrial cancer. *Int J Biochem Cell Biol*. 2019;109:17–22.
38. Chen Y, Song Y, Mi Y, Jin H, Cao J, Li H, et al. microRNA-499a promotes the progression and chemoresistance of cervical cancer cells by targeting SOX6. *Apoptosis*. 2020;25(3–4):205–16.
39. Chen L, Xie Y, Ma X, Zhang Y, Li X, Zhang F, et al. SOX6 represses tumor growth of clear cell renal cell carcinoma by HMG domain-dependent regulation of Wnt/ β -catenin signaling. *Mol Carcinog*. 2020;59(10):1159–73.
40. Kurtsdotter I, Topcic D, Karlén A, Singla B, Hagey DW, Bergsland M, et al. SOX5/6/21 prevent oncogene-driven transformation of brain stem cells. *Cancer Res*. 2017;77(18):4985–97.
41. He Y, Davies CM, Harrington BS, Hellmers L, Sheng Y. CDCP1 enhances Wnt signaling in colorectal cancer promoting nuclear localization of β -catenin and E-cadherin. *Oncogene*. 2020;39(1):219–33.
42. Hu C, Zhang M, Moses N, Hu CL, Polin L, Chen W, et al. The USP10-HDAC6 axis confers cisplatin resistance in non-small cell lung cancer lacking wild-type p53. *Cell Death Dis*. 2020;11(5):328.
43. Zhong Z, Virshup DM. Wnt signaling and drug resistance in cancer. *Mol Pharmacol*. 2020;97(2):72–89.
44. Yu C, Chen F, Wang X, Cai Z, Yang M, Zhong Q, et al. Pin2 telomeric repeat factor 1-interacting telomerase inhibitor 1 (PinX1) inhibits nasopharyngeal cancer cell stemness: implication for cancer progression and therapeutic targeting. *J Exp Clin Cancer Res*. 2020;39(1):31.

Ready to submit your research? Choose BMC and benefit from:

- fast, convenient online submission
- thorough peer review by experienced researchers in your field
- rapid publication on acceptance
- support for research data, including large and complex data types
- gold Open Access which fosters wider collaboration and increased citations
- maximum visibility for your research: over 100M website views per year

At BMC, research is always in progress.

Learn more biomedcentral.com/submissions

